

Spectral hole burning and holography. V. Asymmetric diffraction from thin holograms

Stefan Bernet, Bern Kohler, Alexander Rebane, Alois Renn, and Urs P. Wild

Physical Chemistry Laboratory, Swiss Federal Institute of Technology, ETH-Zentrum, CH-8092 Zürich, Switzerland

Received January 2, 1992; revised manuscript received February 26, 1992

Thin holograms with novel diffraction properties were created in spectral hole-burning materials. Simultaneously sweeping the frequency of the recording light and the phase of the holograms results in an asymmetric distribution of diffraction efficiency between positive and negative orders. Experiments were performed that demonstrate amplified or attenuated diffraction efficiency with respect to holograms recorded at a single frequency. The observed diffraction is well described by a simple model in which small grating amplitudes and weak burning are assumed.

1. INTRODUCTION

Spectral hole burning¹⁻³ (SHB) presents new prospects for high-density optical information storage⁴⁻⁶ and information processing.^{7,8} Holography permits parallel recording and readout of data and is believed to be a promising technique for implementing frequency-selective optical data storage. In holographic hole burning⁹ two crossed laser beams, an object and a reference beam, bleach out a narrow frequency-domain hole in an inhomogeneously broadened absorption band. During reconstruction diffraction occurs from this spatial fringe pattern only if the readout laser frequency matches the frequency of the burned hole.⁹⁻¹¹ The holographic method has been described in detail in previous papers.¹¹⁻¹⁵ For the multiple storage of holograms an additional experimental parameter, the hologram phase, has to be considered. Judicious choice of the relative phases permits control of the interference between the holograms^{13,14} and can even be used to implement parallel logic by the coherent superposition of holograms.⁷

In time-domain holography a SHB hologram is recorded with short light pulses. A time delay between the recording pulses introduced, for example, through a difference in optical paths lengths, results in signal reconstruction from the hologram either in the positive or in the negative (conjugate) diffraction orders, depending on the temporal ordering of the pulses.¹⁶⁻¹⁸ The temporal separation of the pulses is recorded as a spectral modulation of the hole depth, while the temporal ordering of the diffracted pulses affects the hologram phase. Since frequency and time are not independent variables,¹⁹ photon echoes can be programmed by using a tunable cw laser²⁰ to write a spectral pattern into an inhomogeneously broadened spectrum. The spectral pattern corresponds through the Fourier transform to an accumulated photon-echo signal and can be read out with a short light pulse.²⁰

Results from experiments performed with cw lasers indicate that diffraction efficiencies become asymmetric when phase shifts of $\pm\pi/2$ are adjusted between spectrally adjacent holograms, implying that temporal causality effects are also observable in cw experiments.^{13,21} In a pre-

vious paper²² the causality property of SHB holograms was investigated experimentally. The spectral profile of a hologram was broadened by tuning a single-mode dye laser over a small wavelength range (1 cm^{-1}) during the burning process. The efficiency of the holographic image reconstructed by a cw laser beam was substantially modified by introducing a time delay with a glass block alternately placed in the object beam or in the reference beam.

Our motivation in this paper is to investigate the relation between the hologram phase and the distribution of the diffraction efficiency into different diffraction orders for spectrally broad holograms. Experimental data are presented for holograms created by sweeping the laser frequency during burning while simultaneously sweeping the phase of the hologram to simulate the effect of an optical delay. The experimental results are compared with data calculated from a simple model of diffraction from thin holograms recorded in frequency-selective materials in the low-modulation limit and with linear burning assumed.

2. THEORY AND SIMULATIONS

The diffraction properties of spectrally adjacent holograms depend on the relative phase of the holograms.¹³ If a hologram is recorded by sweeping the frequency continuously over an interval of several homogeneous linewidths, then the hologram phase as a function of the frequency strongly determines the diffraction properties. Here we investigate the diffraction properties of plane-wave holograms when the phase is varied linearly with the recording frequency.

The interference pattern of two plane waves of equal intensities, $I_{\text{obj}} = I_{\text{ref}} = I_0/2$, propagating symmetrically about the z axis, with propagation vectors $(k_x, 0, k_z)_{\text{obj}}$ and $(-k_x, 0, k_z)_{\text{ref}}$ with $(k_x^2 + k_z^2)^{1/2} = 2\pi/\lambda = \omega/c$, is described by

$$I(x) = I_0 \left[1 + \cos\left(\frac{2\pi}{\Lambda}x + \varphi\right) \right]. \quad (1)$$

The fringe spacing, $\Lambda = \pi c/(\omega \sin \theta)$, is determined by the

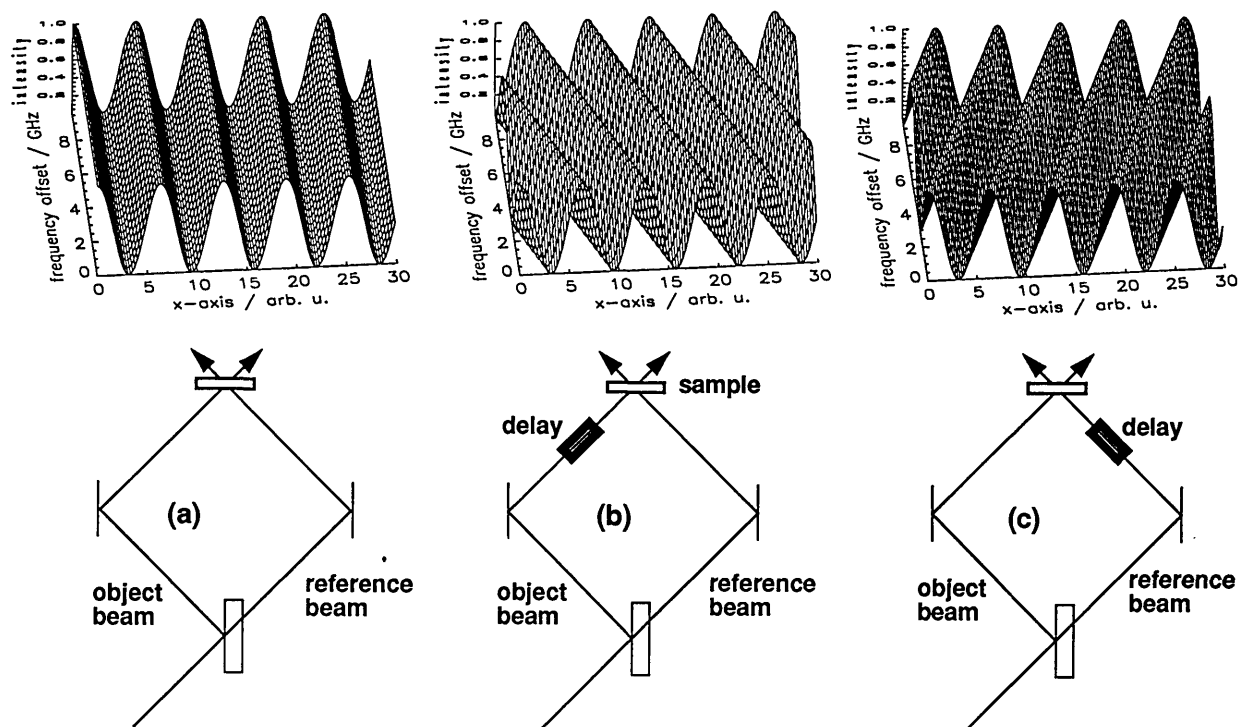


Fig. 1. Interference patterns of plane waves, illustrating the influence of an optical delay on the phase of a hologram. (a) Without the delay the hologram phase is independent of the laser frequency. If (a) the delay is in the object beam, the grating phase moves to the $-x$ direction when the frequency is increased, whereas (c) it is shifted to the $+x$ direction when the delay is in reference beam. Such slanted gratings result in asymmetric diffraction efficiencies. [The phase dispersion shown in (b) and (c) corresponds to an optical delay of approximately 6 cm.]

angle between the interfering beams, 2θ , and the laser frequency ω , and c being the speed of light. The spatial position of the grating is described by the phase φ and depends on the relative phase of the interfering beams.

For spectrally selective recording materials we must consider the effects of varying the recording frequency over a range of several gigahertz. If the frequency of the laser is changed, the fringe spacing changes by the same relative amount, $\Delta\Lambda = \Lambda(\Delta\omega/\omega)$. In the experiments described below $\Delta\omega/\omega$ is of the order of 10^{-5} , so the change in fringe spacing can be neglected.¹³ More important is the change in the spatial phase of the interference pattern. The phase depends on the frequency, if the two interfering beams have different path lengths from the point of beam division to the sample. The spatial shift of the fringes, $\Delta\varphi = (\Delta\omega/c)l$, is proportional to the path difference, l . Figure 1 illustrates how a delay placed in the object beam or the reference beam influences the grating phase. The direction of the shift of the interference fringes, and thus the asymmetry in the gratings shown in Figs. 1(b) and 1(c), depends on which of the two interfering beams has the longer optical path. If the object beam is delayed [Fig. 1(b)], the interference pattern moves in the negative x direction as the recording frequency is increased. Correspondingly, when the reference beam is delayed, the interference pattern moves in the positive x direction, as shown in Fig. 1(c). Whereas in conventional recording materials such a grating is washed out (because of the superposition along the frequency axis), spectral selectivity permits the complete recording.

We now evaluate the diffraction from a thin plane-wave hologram recorded in a frequency-selective material by

continuously varying the frequency between ω_1 and ω_2 . The phase of the spatial fringe pattern is simultaneously changed as a linear function of frequency. The SHB material records frequency-dependent spatial modulations of the absorption coefficient and the refractive index. The amplitude of the optical field directly behind a thin hologram plate can be derived from the amplitude and the phase transmittance function of the sample.²³ For a small grating amplitude, it is proportional to the reference beam amplitude multiplied by the transmittance function^{23,24}:

$$E = E_0 \exp[i(-k_x x)] \exp\left(-i \frac{\hat{n}_0 \omega d}{c \cos \theta}\right) \times \left[1 + \frac{\hat{n}_1 \omega d}{2c \cos \theta} \cos\left(\frac{2\pi}{\Lambda} x + \varphi\right)\right]. \quad (2)$$

\hat{n}_0 and \hat{n}_1 are the zero- and first-order Fourier coefficients of the complex index of refraction, describing amplitude and phase properties of the hologram, and $d/\cos \theta$ is the effective path length through the sample. Equation (2) can be written as

$$E = E_0 \exp[i(-k_x x)] \exp(-i\hat{n}_0) \times \{1 + (\hat{n}_1/2) [\exp(iKx) \exp(i\varphi) + \exp(-iKx) \exp(-i\varphi)]\}. \quad (3)$$

For simplicity, the factor $\omega d/(c \cos \theta)$ has been omitted. Equation (3) describes the near field of three plane waves with propagation vector components $-k_x$, $-k_x + K$, and $-k_x - K$ in the x direction, corresponding to the reference beam, the object beam (+1 diffraction order), and the x component of the conjugate beam (-1 diffraction order),

with K being the grating vector, $K = 2\pi/\Lambda = 2k_x$. Note that the phase of the hologram appears in the diffracted waves in the term $\exp(i\varphi)$, and, most importantly, the phase of the hologram appears with opposite signs in the different diffraction orders.

To describe the frequency dependence of the diffracted field, we assume that the hologram is composed of holograms of continuously varying burning frequencies, and we take the corresponding phase change into account. We restrict ourselves to the calculation of the +1 diffraction order. For recording at a single frequency ω_B and using the frequency-dependent modulation amplitudes as given in Ref. 11, the modulation amplitude of the complex index of refraction for low burning fluences can be written as

$$\hat{n}_1(\omega) = n_1(\omega) - i\kappa_1(\omega) = C \frac{1}{\pi} \frac{1}{\omega_B - \omega + i(\Gamma/2)}, \quad (4)$$

where Γ is the hole width and the constant $C = (N_0\Phi\sigma^{-2}It)$ contains the frequency-independent parameters, such as the absorption cross section σ , the burning fluence It , the photochemical quantum yield Φ , and the initial concentration of the molecules, N_0 .

If, during recording, the frequency ω_B is swept over the range $[\omega_{B1}, \omega_{B2}]$ in combination with a phase sweep range $[\varphi_{B1}, \varphi_{B2}]$, the frequency dependence of the field amplitude diffracted into the +1 order becomes

$$E_1(\omega) \propto \frac{1}{\omega_{B2} - \omega_{B1}} \int_{\omega_{B1}}^{\omega_{B2}} \hat{n}_1(\omega, \omega_B) \exp[i\varphi(\omega_B)] d\omega_B. \quad (5)$$

For a phase that varies linearly with the recording frequency a constant dispersion factor ϕ can be introduced:

$$\phi = \frac{\varphi_{B2} - \varphi_{B1}}{\omega_{B2} - \omega_{B1}}, \quad (6)$$

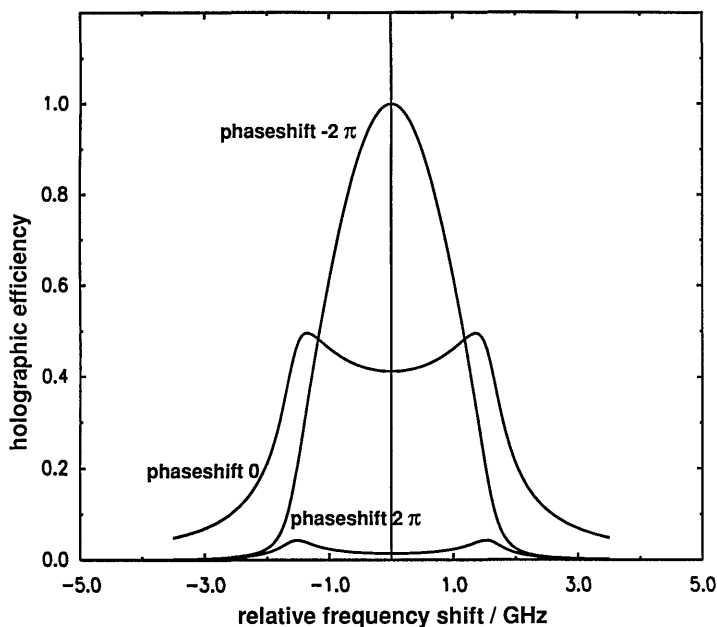


Fig. 2. Calculated hologram efficiency (+1 diffraction order) of holes recorded with different phase shifts. The holes are burned over a range of 3.5 GHz with phase shifts of -2π , 0, or 2π (the hole width is assumed to be 1 GHz). When the conjugate (-1) diffraction order is investigated, exactly the reverse behavior is found.

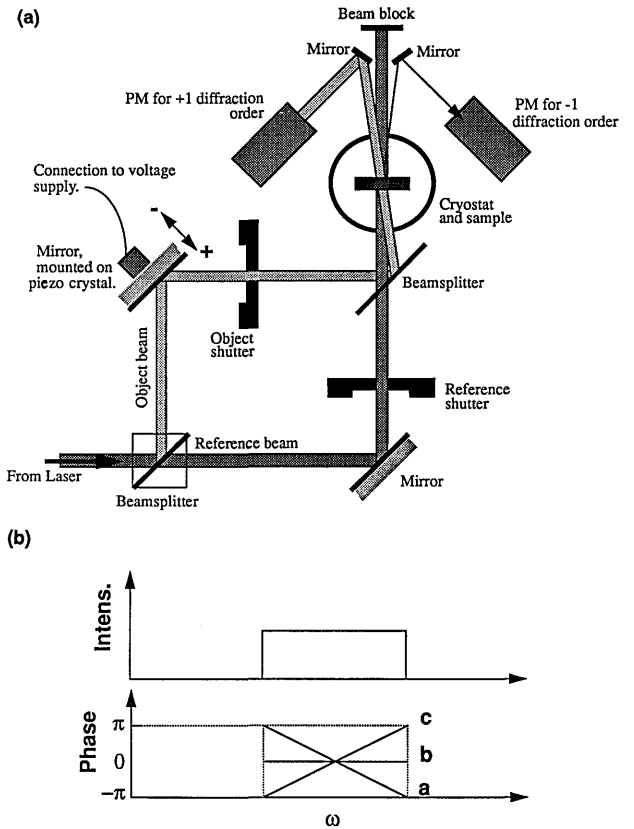


Fig. 3. (a) Schematic illustration of experimental arrangement for thin hologram recording and reconstruction of the ± 1 orders. The effect of a path difference is created by the mirror mounted on the piezoelectric transducer. (b) Frequency and phase sweeps applied during recording of the holograms.

and the phase is given by $\varphi(\omega_B) = \varphi_{B1} + \phi(\omega_B - \omega_{B1})$. By using the complex exponential integral function Ei , defined as the principal value of the integral

$$Ei(z) = - \int_{-z}^{\infty} \frac{e^{-t}}{t} dt, \quad (7)$$

Eq. (5) can be solved analytically:

$$E_1(\omega) \propto C \frac{\exp\{\phi[(\Gamma/2) + i\omega]\}}{\pi(\omega_{B2} - \omega_{B1})} \times \left(Ei \left\{ \phi \left[-\frac{\Gamma}{2} + i(\omega_B - \omega) \right] \right\} \Big|_{\omega_{B1}}^{\omega_{B2}} \right). \quad (8)$$

The wavelength dependence of the hologram efficiency can then be calculated by taking the absolute square of $E_1(\omega)$, given by relation (8). In Fig. 2 $|E_1(\omega)|^2$ is plotted for the +1 diffraction order, with ϕ calculated from Eq. (6) from the burning range (3.5 GHz) with applied phase shifts of -2π , 0, and 2π . A value of $\Gamma = 500$ MHz was assumed. For a negative shift, corresponding to a delay of the object beam, a considerable enhancement of the hologram efficiency is observed with respect to the signal obtained for constant phase. However, the diffraction is strongly suppressed when a phase shift of positive sign, corresponding to a delay of the reference beam, is applied. According to Eq. (3) the efficiency of the negative (conjugate) diffraction order can be calculated by changing the sign of the dispersion factor ϕ in relation (8).

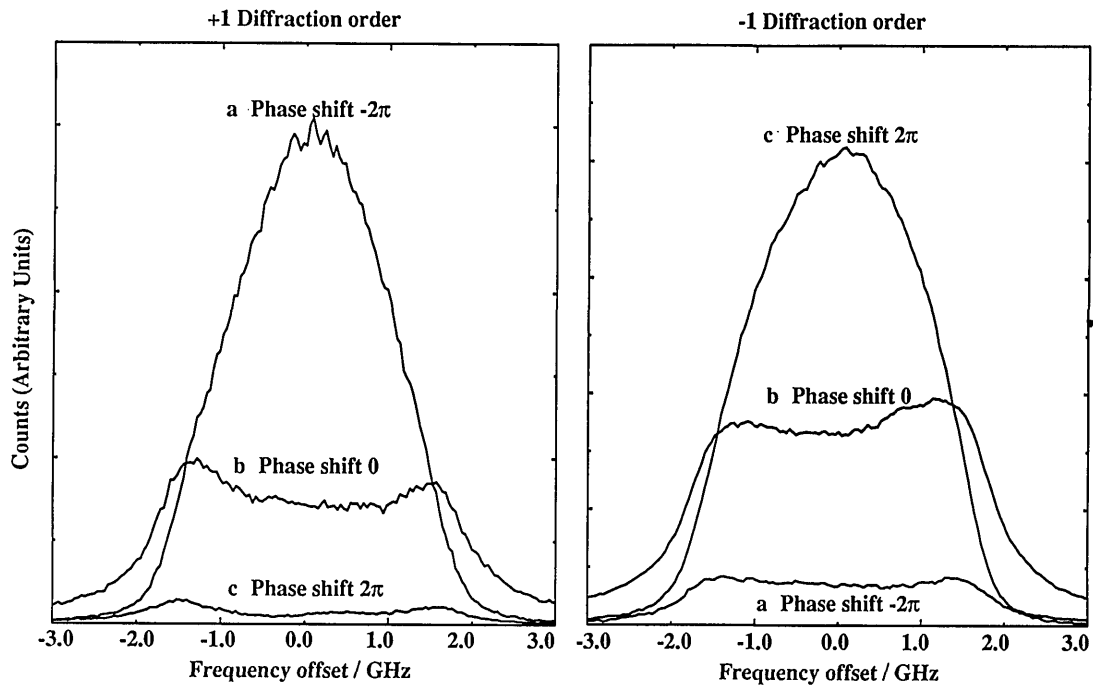


Fig. 4. Hologram efficiency spectra for the different phase shifts applied during burning. The negative phase shift results in an amplification of the hologram efficiency in the first order and attenuation in the -1 (conjugate) order, whereas the positive phase shift leads to the opposite result. Burning with a constant phase results in a symmetric distribution of the diffraction efficiency.

Thus the signals in the -1 diffraction order correspond to the signals in the $+1$ order (Fig. 2) but with the sign of the phase shift reversed.

The results show that applying a phase shift leads to amplification of one diffraction order and attenuation of the other. The suppression of one diffraction order and the increase of the conjugate order becomes more pronounced the larger the ratio of the burning range to the homogeneous linewidth becomes, assuming that a total phase shift of 2π is always used. If a phase shift of more than 2π is applied, then the spectral structure shows more extrema, while the qualitative behavior of the reconstructed signal is not affected.

3. EXPERIMENTS

Experiments were performed to verify the predictions made in Section 2 (Fig. 2). Holograms were recorded in a polyvinyl butyral film doped with chlorin (2,3-dihydroporphyrin) as described elsewhere.¹⁰ The concentration was chosen to give an optical density of 1.6 at the maximum of the $S_1 \leftarrow S_0$ absorption band. Polyvinyl butyral was chosen as a host material because samples of excellent optical quality can be prepared and because of the narrow homogeneous linewidth of the $S_1 \leftarrow S_0$ transition (160 MHz at 1.7 K, Ref. 10). The thickness of the polymer film used was 65 μm .

The experimental setup is illustrated in Fig. 3. A single-frequency dye laser (Coherent 899-29) is pumped by a cw argon-ion laser. The frequency scanning is controlled by software programmed to run the autoscanner laser remotely from a SUN 4/330 workstation via an IEEE-488 interface. The workstation controls all important aspects of the experiment, such as opening and closing the shutters, setting exposure times, and sweeping the hologram phase. Holograms were recorded by dividing

the output of the dye laser into object and reference beams, using a 50% beam splitter. Before splitting the dye laser beam was expanded by a telescope. The beams were overlapped at an angle of 1.5° , resulting in a grating period of 20 μm . A phase shift, linear with the burning frequency, could be created either by insertion of a glass block into one of the recording beams²² or by using a scheme that permits greater flexibility in adjusting the relative phase difference between the two beams and hence of the spatial phase of the hologram. The path length of the reference beam could be changed by applying a voltage to a piezoelectric translator supporting a mirror. A controlled change of an order of an optical wavelength could be easily achieved, permitting the relative phase difference of the two recording beams to be changed. An optical path-length change of δl results in a relative phase shift of $\Delta\phi = 2\pi\delta l/\lambda$.

The optical path lengths of the reference and the object beams were adjusted to be equal to within a few millimeters. The optical delay, either positive or negative, was simulated by moving the piezo-mounted mirror in the object beam under computer control during the burning process. This technique permits the adjustment of arbitrary delay values between the writing beams through the phase dispersion.

The phase shift is considered to be positive if the object path is decreased. In our experiments the scan width during burning of the holograms was in the range of 3.5 GHz, which is approximately seven times the typical hole width of 500 MHz. During burning the laser frequency and the hologram phase were synchronously swept as shown in Fig. 3. For readout of the hologram the object beam was blocked and the reference beam was attenuated by a factor of 50 by inserting a neutral-density filter. The hologram efficiency was measured as a function of the readout frequency.

4. RESULTS AND DISCUSSION

Figure 4 presents experimental results of the frequency dependence of the diffracted signals in both diffraction orders for holograms burned with three different phase sweeps corresponding to (curves a) a negative phase shift, (curves b) a constant phase, and (curves c) a positive phase shift of the object beam. The frequency scan width during burning of the holograms was 3.5 GHz, and the phase changes were (curves a) -2π and (curves c) 2π . These values correspond to a path-length difference of 8.7 cm or an optical delay of 290 ps. A value of 2π was chosen because the amplification and the attenuation obtained in the different diffraction orders are most pronounced for this phase shift. The experimental data clearly demonstrate that the diffraction efficiency between the different diffraction orders can be redistributed by applying an appropriate phase shift and simultaneously sweeping the laser frequency during recording. A strong suppression (>10) of one of the diffraction orders with respect to the other order was observed. Good agreement between the experimental data and the simulated diffraction efficiency according to relation (8) was achieved. The frequency dependence of the signals diffracted into the $+1$ and -1 orders agrees nicely with the shape predicted by the theory, demonstrating that the approximations of weak burning and of small hologram efficiency ($<1\%$) are valid.

In conclusion, these experiments show that control of the grating phase opens a way to increase the absolute diffraction efficiency of mixed holograms stored in SHB media beyond the value obtainable for conventional holographic recording media. Note also that the diffraction efficiency in the wings of the swept signal (curves a) falls off much faster than that of the unswept signal (curves b). This effect can be used to reduce cross talk between holograms recorded at different frequencies, which is essential for spectrally selective data storage. The experimental results presented here show that hole-burning media, because of their high frequency selectivity, permit the recording of new types of holograms and that the hologram phase is a new and important variable, opening a new field of experiments in optics.

ACKNOWLEDGMENTS

We thank P. Nyffeler, W. Jäggi, and M. Traber for valuable support with electronic hardware. We also thank

Petra Kohler and Guido Grassi for synthesizing chlorin. This work was supported by the Swiss National Science Foundation.

REFERENCES

1. B. M. Karlamov, R. I. Personov, and L. A. Bykovskaya, *Opt. Commun.* **12**, 191 (1974).
2. A. A. Gorokhovskii, R. K. Kaarli, and L. A. Rebane, *JETP Lett.* **20**, 216 (1974).
3. W. E. Moerner, *Persistent Spectral Hole Burning: Science and Applications* (Springer-Verlag, Berlin, 1988).
4. A. Szabo, "Frequency selective optical memory," U.S. Patent 3,896,420 (July 22, 1975).
5. G. Castro, D. Haarer, R. M. Macfarlane, and H. P. Trommsdorff, "Frequency selective optical data storage system," U.S. Patent 4,101,976 (July 18, 1976).
6. U. P. Wild, S. E. Bucher, and F. A. Burkhalter, *Appl. Opt.* **24**, 1526 (1985).
7. U. P. Wild, A. Renn, C. De Caro, and S. Bernet, *Appl. Opt.* **29**, 4329 (1990).
8. A. Rebane and O. Ollikainen, *Opt. Commun.* **83**, 246 (1991).
9. A. Renn, A. J. Meixner, U. P. Wild, and F. A. Burkhalter, *Chem. Phys.* **93**, 157 (1985).
10. A. J. Meixner, A. Renn, S. E. Bucher, and U. P. Wild, *J. Phys. Chem.* **90**, 6777 (1986).
11. A. Meixner, A. Renn, and U. P. Wild, *J. Chem. Phys.* **91**, 6728 (1989).
12. R. Locher, A. Renn, and U. P. Wild, *Chem. Phys. Lett.* **38**, 405 (1987).
13. A. Renn, A. J. Meixner, and U. P. Wild, *J. Chem. Phys.* **92**, 2748 (1990).
14. A. Renn, A. J. Meixner, and U. P. Wild, *J. Chem. Phys.* **93**, 2299 (1990).
15. C. De Caro, A. Renn, U. P. Wild, and L. W. Johnson, *J. Lumin.* **50**, 309 (1991).
16. P. Saari, R. K. Kaarli, and A. K. Rebane, *Sov. J. Quantum Electron.* **15**, 443 (1985).
17. P. Saari, R. Kaarli, and A. Rebane, *J. Opt. Soc. Am. B* **3**, 532 (1986).
18. A. Rebane and R. Kaarli, *Chem. Phys. Lett.* **101**, 317 (1983).
19. T. W. Mossberg, *Opt. Lett.* **7**, 77 (1982).
20. M. Mitsunaga and N. Uesugi, *Opt. Lett.* **15**, 195 (1990).
21. K. Holliday, C. Wei, A. J. Meixner, and U. P. Wild, *J. Lumin.* **48/49**, 329 (1991).
22. A. Rebane, S. Bernet, A. Renn, and U. P. Wild, *Opt. Commun.* **86**, 7 (1991).
23. R. J. Collier, C. B. Burckhardt, and L. H. Lin, *Optical Holography* (Academic, Orlando, Fla., 1971).
24. J. Gaskill, *Linear Systems, Fourier Transforms and Optics* (Wiley, New York, 1978).